

Land use Land cover change Assessment at Cement Industrial area using Landsat data-hybrid classification in part of YSR Kadapa District, Andhra Pradesh, India

C. Venkata Sudhakar¹, G.Umamaheswara Reddy^{*2}

Submitted: 29/07/2021 Accepted : 02/02/2022

Abstract: India is the world's second-largest cement manufacturer. It is a significant contributor to the Indian economy's GDP. Kadapa district is one of Andhra Pradesh's largest cement producers. Limestone and cement plant sediment and mine have local, regional, and global impacts on soil, vegetation, and water and air quality. As a result, mapping and change evaluation of the mining area are critical for the sustainability of the cement industry. With today's advancements in remote sensing technology, mapping the Earth's characteristics, observing environmental changes, and controlling natural resources become more efficient with less human efforts than conventional methods. Proposed work focused on land environment temporal change assessment in YSR kadapa district, Andhra Pradesh, India over a period from 1991 to 2019. The results of Landsat-5/7/8 image Hybrid classification using ERDAS IMAGINE and ArcGIS over the study area 684KM² showing an overall accuracy 92 % and kappa index 0.9 in comparison to conventional methods of classification.

Keywords: Cement Industrial area, Landsat data, Land use/cover, Hybrid classification, Indices

This is an open access article under the CC BY-SA 4.0 license.
(<https://creativecommons.org/licenses/by-sa/4.0/>)

1. Introduction

The increasing population, Town/village sprawl, rapid industrialization and growth in infrastructure during the past three decades the demand for Limestone was increased. Limestone is the principal raw material for cement production and construction sector, it is also be used as flux in metallurgical processes, used for manufacturing of calcium carbide, bleaching powder, sugar refining, in fertilizers as soil conditioning agent (http://environm.enticlearance.nic.in/writereaddata/online/TOR/26_Jul_2019_122208490PGAMQLATpfr8.pdf).

Cement plants and Limestone mines in kadapa district contributing a great part to Local people and government of Andhra Pradesh revenue. Cement production and unsupervised Limestone mining activity causes to incredible dynamics in land environment and affecting long-term socioeconomic factors [1]. To balance economic benefits, environment degradation of cement industries and limestone mining, Local Government has to monitor the Land-Environment management approaches of cement industries and limestone mines periodically. Now a day's advances in Remote Sensing technology and image processing techniques could help accomplish the task effectively and efficiently [1, 3, 4, 12, and 19].

1.1. Limestone and cement production in India

India is the world's second-largest cement manufacturer; accounting for over 8% of global installed capacity in 2019. It is a

vital part of the Indian economy. The production capacity of cement in India reached 329 million tonnes (MT) in FY20 and is expected to cross 381 MT by FY22. Fig.1 shows Limestone and Cement production volume in million metric tonnes in India from financial year 2012 to 2020(<https://www.ibef.org/industry/cement-india.aspx>).

Limestone extraction and exploration, as well as its use in cement manufacturing, have a significant effect on climate change and the environment. Natural resource loss, soil, water, and air pollution, landscape changes, and agricultural destruction are only a few examples. As a result, in the mining industry, climate and environmental sustainability are critical [19].

In 2001, the International Council on Mining and Metals (ICMM) developed principles for the mining industry's long-term sustainability (<https://www.icmm.com/mining-principles>).

Sustainable mining practices include Economic development, an Environmental leading practices, Safety excellence, Optimum resource utilization, Community engagement and support. These principles and practices ingrained in the mining industry to ensure sustainable mining as well as prevention of environmental degradation [20-21].

1.2. Literature review

Dalil et al. 2017 [14] used supervised classification with ILWIS 3.3 and Arc GIS 10.2 to study the cement plant and its impact on LULC transition. For the period 2005 to 2015, the Obajana lokoja Local Government Area divided into four classes: built-up, bare surface, vegetation, and water body. Borana et al. 2014 [15] studied the spatial scale and temporal behavior of open pit sandstone mining in and around Jodhpur, Rajasthan, India, as well as LULC changes. This study used IRS-P6, Carto sat, and GeoEye

¹ Department of ECE, Sree Vidyanikethan Engineering College, Tirupati, 517102, India, ORCID ID: 0000-0002-0205-4470

² Department of ECE, S.V.U. College of Engineering, S.V. University, Tirupati, 517502, India,

ORCID ID: 0000-0002-7107-2402

* Corresponding Author Email: sudhakar.chowdam@gmail.com

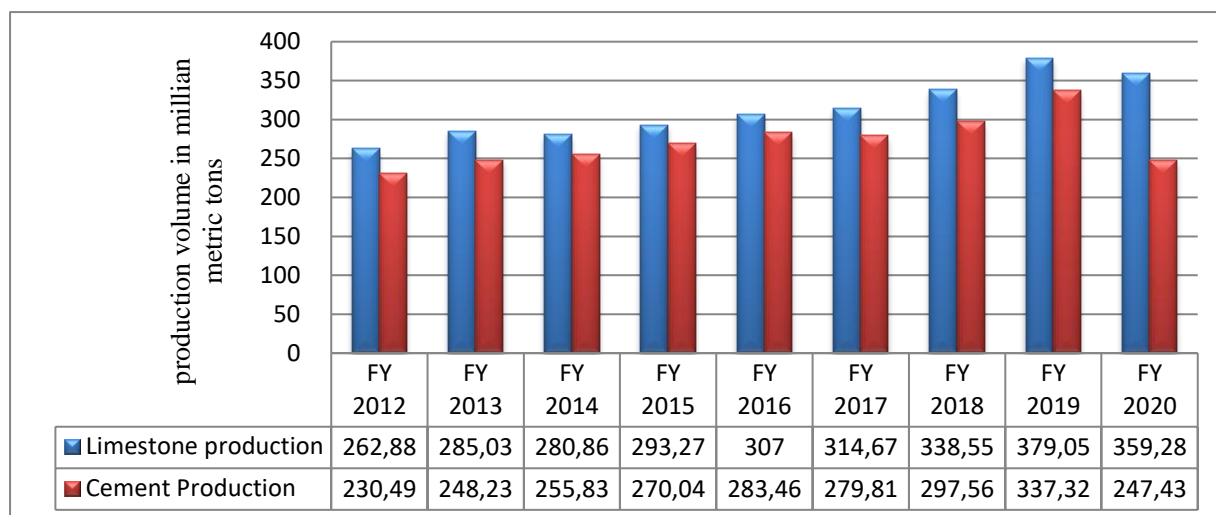


Fig.1. Limestone and Cement production volume in India from financial year 2012 to 2020
(Source: <https://www.statista.com/statistics/669208/india-limestone-production-volume/>)

satellite data, which were processed using ENVI software for the 3D Map and LANDSAT data. The study described vegetation and agricultural areas that are at risk consequently mining operations, scrubland, and vegetation land that has been transformed either into mines and mine overburden, and water sources that have increased consequently of massive sandstone excavation. Pollution of the air, water, and noise level has an effect on the habitation environment. Using Landsat TM data, Rawat et al. 2013, [16] analyzed the LU/LC transition using GIS and the Supervised classification process, computing NDVI, NDWI, and NDBI indices from 1990 to 2010. He came to his conclusion about the LU/LC groups since the built-up area grew from 1.25 km² to 4.08 km², accounting for 8.88 percent of the total area. The area covered by vegetation decreased from 10.29 km² to 7.29 km². Fanan et al. 2014 [17] used multi-temporal satellite images with ILWIS and SPSS to investigate the effect of limestone mining and cement production on vegetation over a 32-year period from 1996 to 2006. The study found that the built-up area increased from 0.05 to 1.51 km², while vegetation decreased from 4.30 to 1.51 km². Are search on remote sensing image classification methods and techniques for enhancing classification accuracy was conducted by [18]. The user's requirements, the economy, the size of the study area, and the analyst's experience all play a role in the decision to use remotely sensed data. The LISS III data from Resourcesat-1/2 in 2005-06 and 2015-16 are used in Production of images. Study area Industrial profile

Major cement industries in YSR kadapa district are, India Cements Limited, Zuari cements, Bharathi Cements in and around the Yerraguntla town located 47km towards west from district headquarters and located between the Geographical Co-ordinates 14.63°N latitude and 78.53°E longitude [19].

Over ¾th of total Limestone in India is producing in Madya

Pradesh, Rajasthan, Tamil Nadu, and Andhra Pradesh, Gujarath, and chattisgarh states. Kadapa district is the one of largest cement producers in Andhra Pradesh with capacity of 11.238 MTPA. The present study is limited to limestone (cement-grade, slab-grade) mines and cement industries land use/cover area mapping and change assessment bounded over the area 684KM² in kadapa district [6, 19] shown in Fig.2.

2. Data collection

Remote sensing is a cost effective, precise technology for mapping the Land use/cover pattern on a varied scale. In 1972, NASA sent the first Landsat satellite into orbit. Because of its long history of earth observation and rich spectral bands with sufficient spectral details, Landsat data is ideal for analysing earth surface features [1]. Landsat satellites provide an enormous wealth of data with high temporal frequency for the scientific analysis and change assessment. Limestone quarry growth or decline rate is slow hence decadal observation carried out (representing years 1991,2001,2011 and 2019) for mapping and land use/cover change assessment of industrial area using LANDSAT images with low cloud coverage in the month of March/April downloading from the US Geological Survey's (USGS) Earth Explorer platform (<https://earthexplorer.usgs.gov>). The study is based on imagery from TM/ ETM+/OLI sensors with a common spatial resolution of 30 meters and six overlapping spectral bands (B, G, R, NIR, SWIR1 and SWIR2). Table 1 indicates Sensor, sensor ID, spacecraft ID, path/raw and the Sun elevation angle at the time of the acquisition of each image. All the images were Level 1T processed (L1TP) and accessible in GeoTIFF format with 30m pixel size and UTM WGS84 map projection.

Table 1. Study area LANDSAT images metadata

Image acquisition date	Sensor	Spacecraft	Path /Row	Sun elevation angle (degrees)	Sun azimuth angle (degrees)
6 th March 2019	OLI_TIRS	LANDSAT_8	143/050	55.87	124.46
1 st April 2011	TM	LANDSAT_5	143/050	60.32	106.98
29 th April 2001	ETM	LANDSAT_7	143/050	64.18	86.55
10 th April 1991	TM	LANDSAT_5	143/050	55.29	97.33

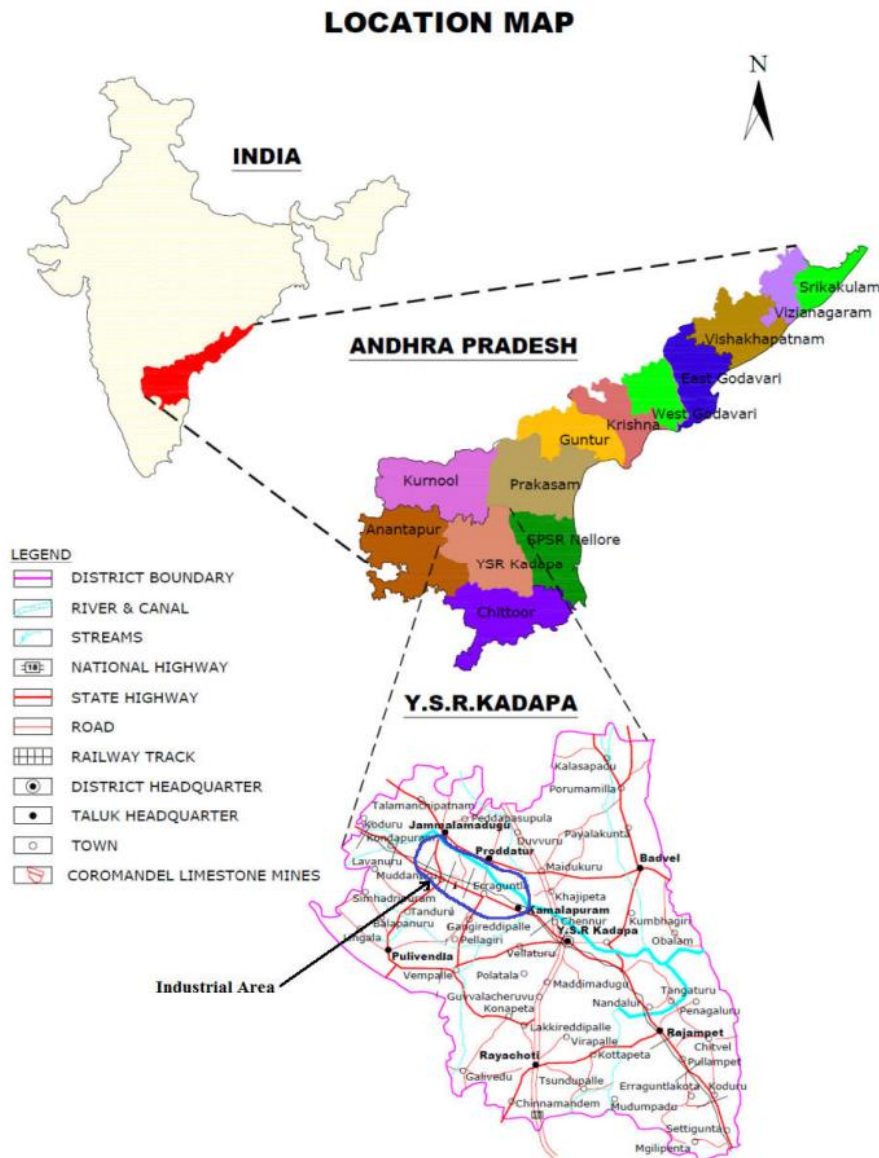


Fig. 2. Cement industrial area Location map in Kadapa District, Andhra Pradesh, India

3. Image Classification

For mapping, the industrial area for decadal change assessment, Classification flow summarized in Fig. 3. The methodology includes Pre-processing, Classification, Change assessment, Accuracy assessment and post classification.

3.1. Pre-processing

Preprocessing operations include atmospheric correction, geometric corrections, radiometric corrections, stacking of image bands. In this study, we are used Level-1 Precision Terrain (L1TP) processed Tier-1 Landsat data. It was systematically, radiometrically, geometrically and topographically corrected using ground control points, the scenes suitable for time series pixel level analysis. The Landsat 5, 7 & 8 images are obtained for the study area were recorded in bands ranging from 1 to 9 for Landsat 8, Bands 1 to 8 for Landsat 7 and Bands 1 to 7 for Landsat 5. In the Landsat8 band 8 does not have color (i.e. Panchromatic) that will help in analyzing the data visually. Landsat 8 individual bands 1 to 7 and 9 (1 to 8 for Landsat 7 and 1 to 7 for Landsat 5) are Layer stacked to form multispectral images which can therefore be viewed in different color combination (RGB combination). Upon careful examinations, band combination NIR-5, Red-4 and Blue-3

for Landsat 8 image and NIR-4, Red-3, Blue-2 for Landsat 5&7 images shown in Table 2. They were used for revealing clearly all the lulc classes on the images. Subset image extracted from multi-band image with the help of industrial area shape file developed in ArcGIS 10.5 for cropping the image [23].

Table 2. Landsat satellites and its Bands

Satellite	Green Band	Red Band	NIR Band	SWIR Band	TIR Band
Landsat_5/7	2	3	4	5,7	6
Landsat_8	3	4	5	6,7	10,11

3.2. Multispectral indices

Understudy of different land surface properties such as vegetation, surface water and Barren land and built-up land (Iswari et al. 2018). We are computed NDVI, NDWI and NDBI indices using equations (1) to (5). Table 3 shows statistical values of indices for the years 1991 and 2019; these values used for extracting training data for Land use-Land cover change analysis (Jensen 2015). No vegetation defined as NDVI values below 0.18, and vegetation defined as NDVI values between 0.19 and 0.48.

Table 3. Indices statistics for the years 1991 and 2019 of the study area

Index	2019					1991				
	Minimum	Maximum	Dynamic range	Mean	Standard deviation	Minimum	Maximum	Dynamic range	Mean	Standard deviation
NDVI	-1.00	0.48	1.48	0.13	0.06	-0.16	0.65	0.81	0.06	0.07
NDBI	-0.32	1.00	1.32	0.05	0.07	-0.5	0.47	0.97	0.31	0.07
NDWI	-1.00	0.32	1.32	-0.05	0.07	-0.47	0.50	0.97	-0.30	0.07
MNDWI	-1.00	0.39	1.39	-0.11	0.06	-0.89	0.51	1.40	-0.43	0.06
BU	0.68	0.52	0.16	0.09	0.06	-0.34	-0.18	0.16	0.18	0.07

$$NDVI = \frac{NIR-Red}{NIR+Red} \quad (1)$$

$$NDWI = \frac{NIR-SMIR}{NIR+SMIR} \quad (2)$$

$$NDBI = \frac{SMIR-NIR}{SMIR+NIR} \quad (3)$$

$$\text{Modified NDWI} = \frac{\text{Green band}-\text{SMIR band}}{\text{Green band}+\text{SMIR band}} \quad (4)$$

$$\text{Built-up Index BU} = NDBI - NDVI \quad (5)$$

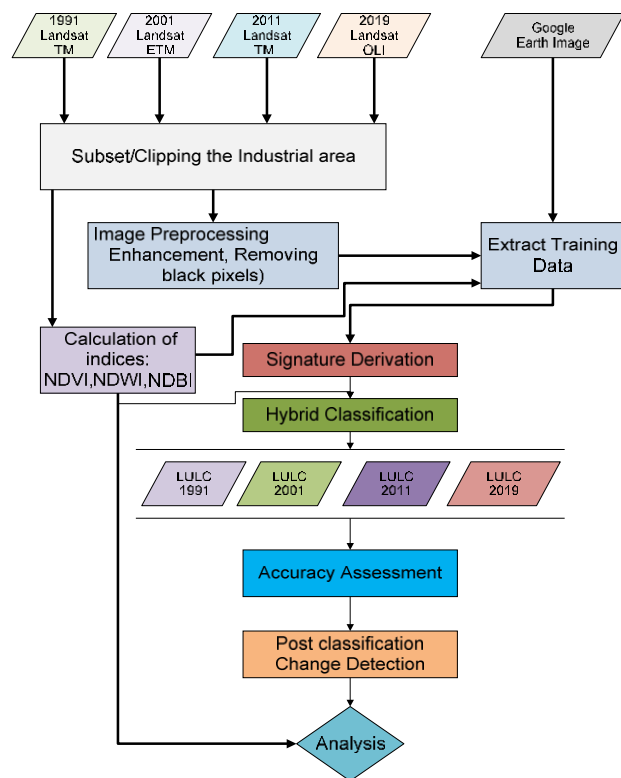


Fig.3. Land use/cover change assessment flow chart

3.3. Image Enhancement

Image enhancement is the process of making important features of raw data more interpretable by increasing the apparent distinction between the features in the scene for a particular application. Spatial enhancement modifies pixel values based on the values of surrounding pixels. Convolution-edge enhancement filters are the most commonly used filters for an image quality enhancement in the spatial domain. Here we are used a 3x3 kernel matrix to average small sets of pixels across an image for deriving the modified DN value to replaces the centre pixel and a 3x3 edge enhancement filter

used to deduce shape information and to extract edges formed by roads, railways and riverbeds.

3.4. Hybrid Classification

Table 4. Industrial area LULC classes in the study area

S. No.	Land use/cover class	Description
1	Limestone Mines/ Quarries	Areas include both Cement Grade and Slab Grade Limestone mining activities with significant surface expression. The main cement grade limestone mines are Thippaluru Limestone Mines(Bharati cements) Zuvari cement Limestone mines Coromandel Limestone Mine (ICL)
2	Mine waste	Mine waste extracted from the Napa slab quarry and cementGrade Limestone mine are dumped close to the quarry and surroundings
3	Town/village/ Roads/Rails	Residential, Non-building structures, systematic street patterns, Transportation such as Roads and Rails and utilities are included in this
4	Industrial area	This area included major cement and power plants like The India Cements Limited (previously Coromandal Cements)-Chilamakur, The India Cements Limited-Yerraguntla, Zuari cements- Yerraguntla, Bharathi Cements Limited-Nallalingayapalli, Rayalaseema Thermal Power Plant (RTPP)
5	Uncultivated land	Uncultivated land also called follow land which is normally used for farming, but this is left with no crops on it for a period in order to let it recover its productiveness.
6	Crop land	Agricultural lands under crop, the main crop lands in this study include rice, groundnut ,vegetables, Bengal gram, red gram etc.
7	Natural vegetation	It include group of plant/tress that are grown naturally without human aid.
8	Barren land/ Hill shade	It included which do not support for any vegetation, 1/3 rd of the area having vegetation or other cover and Hill areas
9	Water bodies	Included reservoirs, Rivers, ponds and significant accumulation of water in Mines
10	Dry-bodies	Dried up water bodies, including man-made lakes, reservoirs and River

A supervised maximum likelihood classification alone exposed a problem caused by spectral confusion in mine waste and barren lands. This problem minimized by using hybrid classification approach. The Hybrid classification approach is more accurate and efficient [10]. The hybrid classification process includes three steps :(1) Unsupervised classification using ISODATA algorithm

for land use-land cover except settlement and Bareland. (2) Supervised maximum likelihood classification for settlement and Bareland and (3) an overlay of the two classifications [(1) + (2)]. Table 4 (<https://kadapa.ap.gov.in/>) describes the 10 Land Use-land cover classes in the Industrial area, YSR Kadapa District, Andhra Pradesh, India. Fig. 4 shows the 10 land use-land cover classes of Satellite Images taken from *Google Earth* [9].

3.4.1. ISODATA Algorithm

The ISODATA (Iterative Self-Organizing Data Analysis) algorithm is an amendment of the k-means clustering algorithm, which includes [22].

- a) If the separation distance between clusters in multispectral feature space is less than a user-defined threshold, the clusters will be merged (Merge two clusters if their distance exceeds a certain threshold).
- b) Split a single cluster into two clusters using rules. (If standard deviation in any one dimension is greater than some threshold, split into two clusters).

It is tedious in nature, passing through the image space set of times before returning to a logical conclusion. When using the ISODATA formula for classification, the analyst is usually required to define the following parameters (Jensen, 2015).

- **Minimum size of the cluster:** The minimum size of a cluster refers to the smallest number of pixels required to form a cluster. If there are less number pixels in a cluster than the minimum size. It's thrown out, and the pixels are assigned to another cluster.
- **Maximum size of the cluster:** The number of that can be contained in a cluster is referred to as the maximum cluster size. If a cluster tends to have more pixels than the cap, those pixels will be shifted to another cluster.
- **Maximum standard deviation (max):** When the standard deviation for a cluster exceeds the given maximum standard deviation and the number of pixels in the class is greater than twice the affirmed minimum pixels in a class, the cluster is split into two clusters. The old class centres -1σ are the mean vectors for the two new clusters.
- **Minimum separation between pairs of cluster:** combine the clusters if they are not separated by a given minimum distance

(less than the weighted distance).

- **Maximum number of clusters:** If the number of clusters reaches the upper limit of K_{max} , the clustering process will be terminated. The maximum percentage of pixels with unchanged class values between iterations is indicated by T . When this K_{max} is reached, the ISODATA algorithm stops working. It's likely that certain datasets will never reach the optimum level of unaltered data. Processing must be stopped and the parameter changed if this happens. If the clusters are not separated by a defined minimum distance, combine them (less than the weighted distance).
- **Minimum number of cluster:** In another scenario, if the cluster's min limit of K_{min} is exceeded, merging the cluster would be prohibited.
- **Maximum number of iterations (M):** If the number of iterations in K-Means clustering exceeds the maximum number of iterations, the method will be terminated.

The algorithm works as follows once all of the user-defined inputs have been supplied to the classifier

(<https://nptel.ac.in/courses/105/103/105103193/>).

- Based on the shortest (mean spectral distance) distance to the middle, assign each pixel to the nearest cluster.
- Recalculate the mean, standard deviation, and distance between cluster centres within each cluster.
 - Split Clusters if one or more standard deviation is greater than the user-defined threshold (standard deviation $>$ some threshold, split into two clusters)
 - Merge Clusters if the distance between them is less than the user-defined threshold (distance between two clusters $<$ some threshold, merge them)
- Perform second iteration with the new cluster centers.
- Clusters with a limited number of pixels should be removed.
- Further iterations are performed until:
 - i. An average inter-center distance is less than the user-defined threshold.
 - ii. If the average change in the inter-center gap between iterations is less than a threshold, the iteration is considered effective.
 - iii. The maximum number of iterations is reached.



(a). Limestone Mine



(b). Mine waste



(c). Town/villages/ Roads/ Rails



(d). Fallow Land



(e).Crop land



(f).Natural vegetation



(g).Barren Land



(h).Water bodies

Fig.4. LULC models from Industrial area using Google earth

3.4.2. Maximum likelihood (ML) classifier

The maximum likelihood (ML) classifier based on the Bayes theorem, is the most commonly used supervised learning method in remote sensing. The ML classifier is a statistical classifier that uses a multivariate normal distribution for the data in - class (Gaussian probability density model).It's a parametric method based on the assumption of a normal distribution class signature. (<https://nptel.ac.in/courses/105/103/105103193/>)This assumption is true in general; however, it is invalid for classes with several subclasses or classes with different spectral features.

- The probability of an image pixel for different training data classes is calculated by an ML classifier, which then assigns the image pixel to the class with the highest likelihood.

To identify the class of an unknown pixel, the highest probability class will be used (image pixel, where we want to classify it or image pixel, which we want to classify it).The conditional probability of a feature vector X to be in the class of C_i is

$$P(C_i/X)$$

- P(C_i/X), is computed using Bayes Theorem in term of P(X/C_i).This is the probability of X to be in the class of C_i

$$P(C_i/X) = \frac{P(X/C_i) P(C_i)}{P(X)}$$

X is assigned to class C_i such that, that maximum probability we will get for C_i class using

$$P(C_i/X), = \text{Max}_i P(C_i/X)$$

Where i = 1 to K (the number of classes)

P(C_i) = the probability of occurrence of the class 'i' in the image
P(X) = the multivariate probability density function of feature X
P(X/C_i), Probability of pixel to be classified in class C_i is considered as Multivariate Gaussian distributed in parametric classifier (http://sar.kangwon.ac.kr/etc/rs_note/rsnote/cp11/cp11-7.htm)

- Gaussian distributions are very simple to handle.

- Each class conditional density function P(X/C_i) is represented by mean vector (μ_i) and covariance Matrix (Σ_i) and this mathematical expression is

$$P(X/C_i) = \frac{1}{2\pi^{L/2} |\Sigma_i|^{1/2}} e^{-\frac{1}{2}(X-\mu_i)^T \Sigma_i^{-1} (X-\mu_i)}$$

The Gaussian distribution is based on the following assumptions:

- An each class is considered to be multivariate normally distributed. This means that each class has a mean with the highest probability of occurrence.
- The likelihood function decreases exponentially as the feature vector X deviates from the mean vector (μ_i).
- The rate of decrease is governed by the class variance: Where smaller the variance steep will be the decrease and larger the variance slower will be the decrease.

$$g_i(X) = -\frac{1}{2}(X - \mu_i)^t \sum_i^{-1} (X - \mu_i) - \frac{L}{2} \ln 2\pi - \frac{1}{2} \left| \sum_i \right| + \ln P(w_i)$$

Covariance matrix for each class are assumed different, Where (X - μ_i)^t Σ_i⁻¹ (X - μ_i) is known as Mahalanobis distance between X and μ_i. Between two multivariate quantities x and y, the Mahalanobis distance is

$$d_m(x, y) = (x - y)^t \sum_i^{-1} (x - y)$$

This classification has a minimum overall probability of error.

$$D = \ln(a_c) - [0.5 * \ln(|cov_c|)] - [0.5 * (X - M_c)^T * (Cov_c^{-1}) * (X - M_c)]$$

Where D is the weighted distance (likelihood); c represents a particular class of interest; X is the vector of spectral signature for the candidate pixel from the testing data; M_c is the mean vector of the sample of class c from the training data; a_c is the percent probability that any candidate pixel is a member of class c; |Cov_c| is the determinant of Cov_c; Cov_c⁻¹ is the inverse of Cov_c; 'ln' is the normal logarithm function and T is the transposition function.

Cov_c is the covariance matrix of the pixels in the sample of class c from the training data (John R. Jensen, 2015).

- Sufficiency (complete information about the parameter of interest contained in its Maximum likelihood estimator(MLE))
- Consistency (For data of sufficiently large samples, the true parameter value that produced the data can be recovered asymptotically.)
- Efficiency (lowest-possible variance of parameter estimates achieved asymptotically).
- Invariance of parameterization (same MLE solution obtained independent of the parameterization used)

3.5. Accuracy assessment

This is an important to have faithful results in precise change detection from outcome of classification of data. Evaluation of the accuracy derived from thematic map. In the classification, checkpoints are courtesan from the Google Earth. Accuracy assessment accomplished by using a supervised Classifier toolbar in ERDAS Imagine 2015. We have taken fifty random ground control points from the Google Earth to measure the accuracy of the classified images of the years 1991, 2001, 2011 and 2019. An error matrix generated and compared the relationship between known reference data (ground truth) and the results of an automated classifier [8]. The proportionate reduction of error generated by a classifier that is expressed by Kappa coefficient. Processed resultant compared with the error of a completely random classifier.

Kappa coefficient computed by the mathematical equation

$$Kappa (K) = \frac{(NXA) - B}{N^2 - B}$$

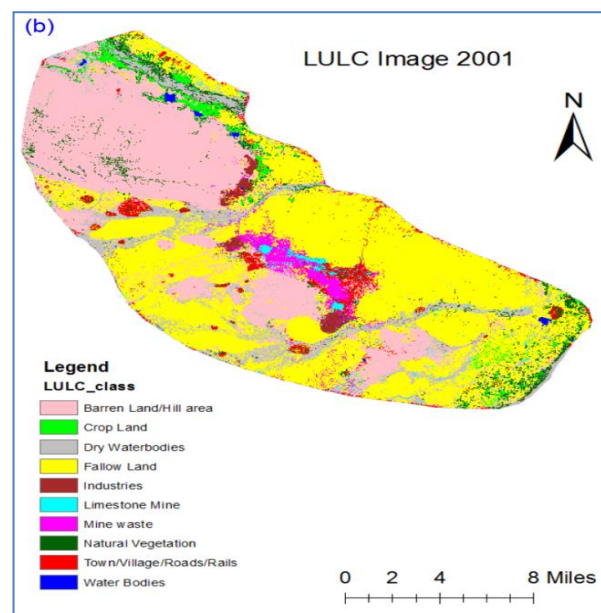
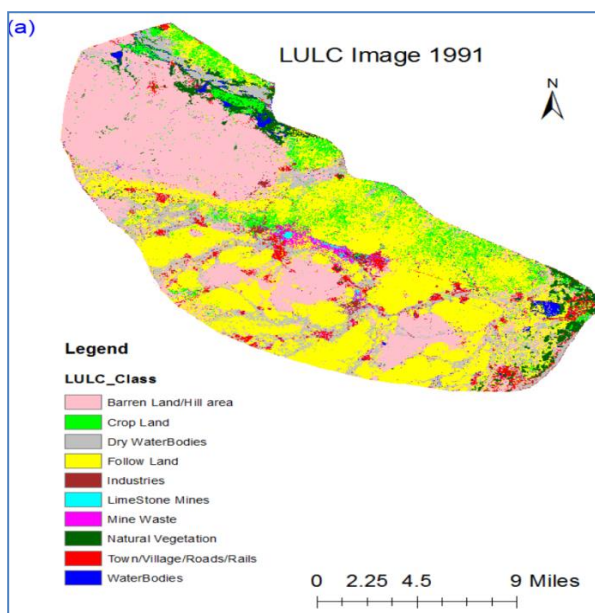
Where N is the total number of pixels used for accuracy assessment, A is the total number of correctly classified pixel; B is the product of total number of ground truth for a class and total number of classified pixel for that class.

3.6. Post-classification change Analysis

Cross tabulation Matrix is prepared with land use/cover pixels at a particular date by cross tabulating with a different date. The change recognition matrix comprise $n \times n$ cells with a land use-land cover change map ‘from 1991 to 2001’. Subsequently ‘from 2001 to 2011’, ‘from 2011 to 2019’ and ‘from 1991 to 2019’ class change matrices of land use-land cover are produced with 10 land use-land cover classes in each image result of 100 possible sequence changes, 10 static elements for each time period. Areal extent and spatial distribution of Land use/cover changes quantified by the pixel-by-pixel operation [10].

4. Results and Discussion

Landsat Multi-Temporal images for the years 1991, 2001, 2011 and 2019 classified to obtain decadal change of the study area using Hybrid classification algorithm approach in the ERDAS 2015. Ten LULC classes of the study demonstrated in the Table 4 and classified map shown in Fig.5. On keen Inspection of the four land use-land cover maps, it revealed that Fallow Land and Barren Land symbolize the highest portion of the study area. Industries, Town/Village/Roads/Rails Land use classes seen to be interrelated. Few water bodies found to be part of Limestone Mine site.



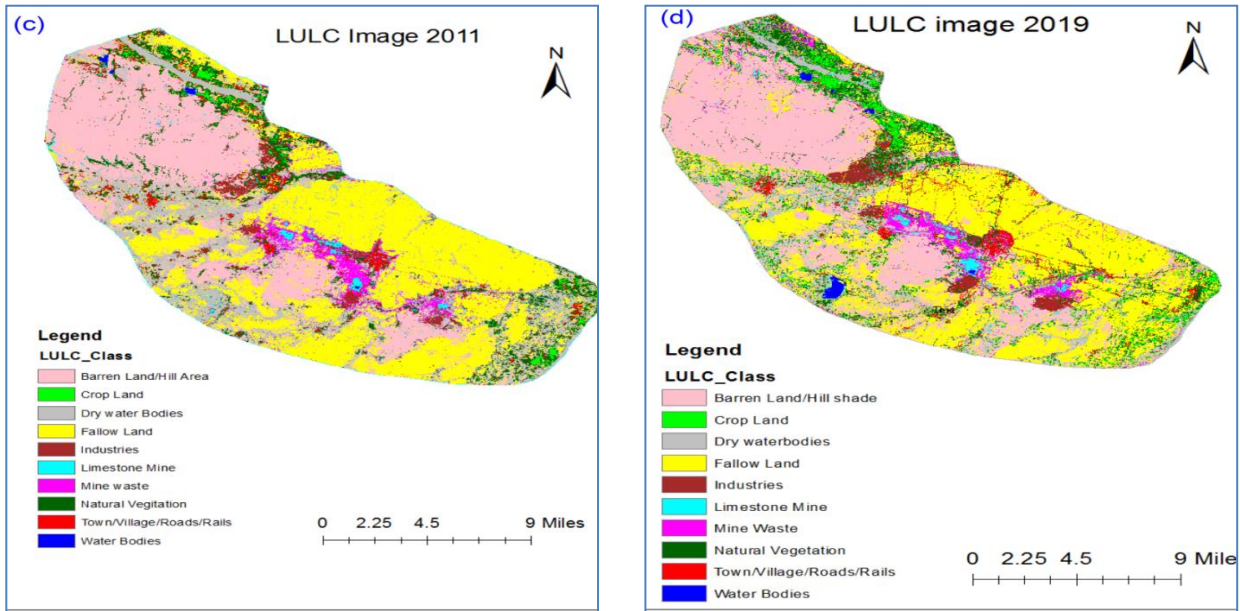


Fig.5. LULC map of Industrial area in 1991, 2001, 2011 and 2019

Table 5 illustrates the areal expansion of the industrial area of the individual LULC categories in square Kilometer (KM²) and their occupation in term of percentage. Bar graph Fig. 6 shows the trends in LULC changes in the four consecutive decadal years 1991, 2001, 2011 and 2019.

Table 5. Land use / cover areal expansion (Total study industrial area is 684 KM²).

land use-land cover class	Area expansion in 1991		Area expansion in 2001		Area expansion in 2011		Area expansion in 2019	
	KM ²	%	KM ²	%	KM ²	%	KM ²	%
Limestone Mines	2.39	0.35	6.28	0.92	9.00	1.32	11.18	1.64
Mine waste	10.50	1.53	16.67	2.44	19.90	2.91	25.56	3.74
Town/Village/Roads/ Rails	21.45	3.14	17.92	2.62	19.25	2.81	17.37	2.54
Industries	5.73	0.84	10.21	1.49	11.09	1.62	12.31	1.80
Fallow Land	261.1	38.17	312.6	45.71	228.6	33.42	227.6	33.28
Crop land	46.64	6.82	13.91	2.03	5.91	0.86	29.12	4.26
Natural vegetation	23.76	3.47	25.25	3.69	54.57	7.98	64.98	9.50
Barren land / Hill shade	226.8	33.16	210.6	30.79	207.9	30.40	228.1	33.35
Water bodies	7.60	1.11	2.94	0.43	0.98	0.14	2.92	0.43
Dry water bodies	78.73	11.51	68.20	9.97	127.4	18.63	64.68	9.46

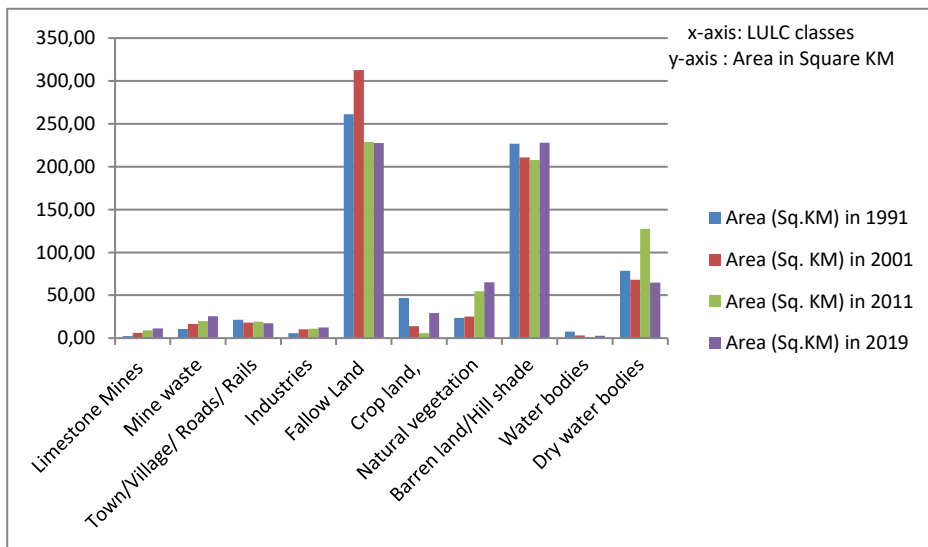


Fig.6. Industrial area Land use/cover dynamics in 1991, 2001, 2011 and 2019 years

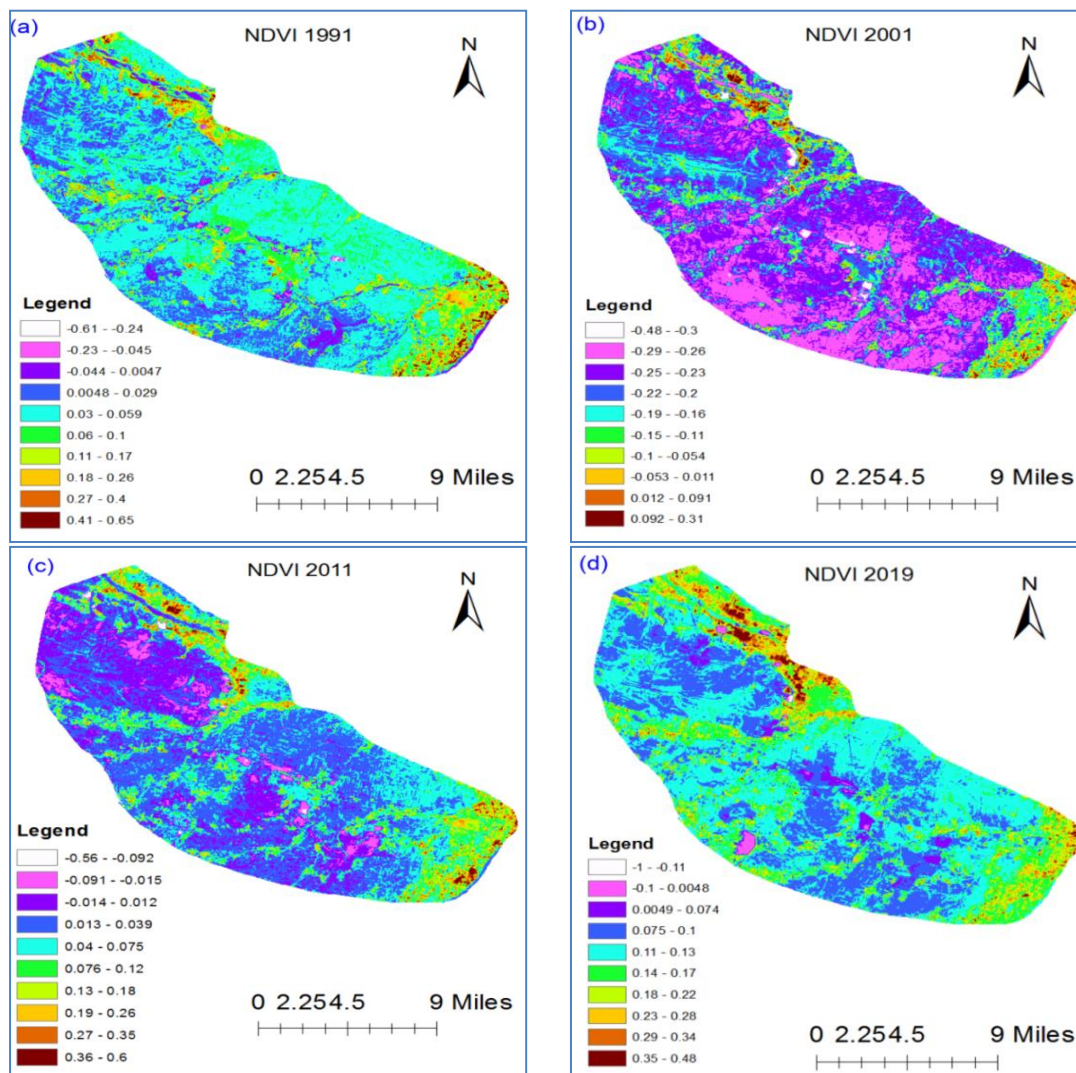


Fig.7. Industrial area NDVI images in the years 1991, 2001, 2011 and 2019

The statistics Table 3 and Fig.7 shows that lesser the NDVI value from range -1 to 0.18 usually represent Water bodies (-0.0175 to -0.328), Built up (-0.019 to 0.060) and Barren land (-0.001 to 0.166). The NDVI value of the vegetation is ranging from 0.19 to 0.48.

4.1. Change Detection Matrix

Change detection matrix constructed to determine change and unchanged land use/cover classes with other classes, using two different dates' thematic maps. This matrix contains crucial data on the extent and spatial distribution of land use changes. This matrix contains crucial data on the extent and spatial distribution of land use changes. In this research work we formed four change detection matrices for the years 1991-2001, 2001- 2011, 2011-2019 and 1991-2019 from four thematic maps using the ArcGIS 10.5 and Microsoft Excel. The Transition matrix diagonal elements represent unaffected land use/cover classes including total area, the off-diagonal elements represent altered land use/cover classes. Elements in the column represent lulc classes of earlier date and elements in the row represent lulc classes of later date [8]. Tables 6-9 show the LULC Transition matrices for 3 decadal changes from 1991 to 2019.

Change detection matrix in Table 6 shows the total Limestone mining in the year 1991 is 2.39KM² but this Limestone mining area in the year 2019 is 11.18KM². To make this 11.18KM² Limestone

mining area in the year 2019, it taken 0.86 KM² from Mine waste, 0.51 KM² from Towns/ villages/Roads/Rails, 0.91 KM² from Industrial are, 3.74 KM² from fallow land, 0.51 KM² from crop land, 0.3 KM² from natural vegetation, 1.69 KM² from barren land, 0.19 KM² from water bodies and 2.78 KM² from Dry water bodies. ICL cement plant in Chilamkur village and another plant in Yerraguntla commissioned in 1998 and 1999 respectively and expanded in 2010, Zuari Cement plant commissioned in 1998 in Krishnanagar which is 7 km away from Yerraguntla town, Bharathi Cement plant established in 2006 at Nallalingayapalli near Yerraguntla and RTPP stage-1(Unit-I)commercial RTPP stage-1(Unit-I)commercial RT As a result of the creation of cement factories, crop and follow-on land have decreased, and the inhabitants in the neighbouring town/village have gained employment.

Table 6. Change detection matrix from 1991 to 2019 in sq.KM

class No.	class Name	Limestone Mines	Mine waste	Town/Village/Roads/Rails	Industrial area	Fallow land	Crop land	Natural vegetation	Barren land/Hill shade	Water bodies	Dry water bodies	Total Area 2019
1.	Limestone Mines	0.41	0.86	0.51	0.19	3.74	0.51	0.30	1.69	0.19	2.78	11.18
2.	Mine waste	0.52	2.64	1.40	0.15	10.22	2.05	0.74	4.43	0.33	3.09	25.56
3.	Town/Village/Roads/Rails	0.28	0.95	2.59	0.36	6.69	0.83	0.32	1.74	0.20	3.41	17.37
4.	Industrial area	0.14	0.40	0.20	1.40	1.50	0.52	0.03	7.20	0.05	0.87	12.31
5.	Fallow land	0.28	1.96	4.03	0.60	151.03	24.35	4.82	20.52	2.17	17.85	227.62
6.	Crop land	0.05	0.18	1.88	0.14	7.98	3.30	5.20	5.67	0.84	3.88	29.12
7.	Natural vegetation	0.24	1.13	5.21	0.56	20.79	7.51	6.39	11.87	1.70	9.59	64.98
8.	Barren land/ill shade	0.19	1.45	2.60	0.75	39.10	4.44	2.50	160.81	0.43	15.84	228.10
9.	Water bodies	0.02	0.06	0.08	0.06	1.40	0.01	0.16	0.10	0.52	0.51	2.92
10.	Dry water bodies	0.25	0.86	2.96	1.50	18.60	3.10	3.30	12.02	1.18	20.91	64.68
Total area 1991		2.39	10.5	21.44	5.71	261.04	46.63	23.76	226.05	7.60	78.72	683.84

Table 7. Change detection matrix from 2011 to 2019 in sq.KM

class No.	class Name	Limestone Mines	Mine waste	Town/Village/Roads/Rails	Industrial area	Fallow land	Crop land	Natural vegetation	Barren land/Hill shade	Water bodies	Dry water bodies	Total Area 2019
1.	Limestone Mines	1.90	1.68	0.54	0.31	1.31	0.03	0.41	1.67	0.07	3.26	11.18
2.	Mine waste	1.09	6.88	1.26	0.34	5.07	0.08	1.68	3.87	0.03	5.26	25.56
3.	Town/Village/Roads/Rails	0.45	1.30	4.81	0.54	3.94	0.02	1.32	0.70	0.01	4.27	17.37
4.	Industrial area	0.20	0.82	0.86	4.82	0.92	0.03	0.98	2.07	0.06	1.56	12.31
5.	Fallow land	0.64	2.69	2.16	1.33	158.00	1.04	8.92	18.41	0.19	34.24	227.62
6.	Crop land	0.04	0.32	1.55	0.14	4.38	2.30	10.47	3.44	0.00	6.48	29.12
7.	Natural vegetation	0.24	2.27	3.83	0.92	13.37	1.51	19.01	7.22	0.03	16.60	64.98
8.	Barren land/Hill shade	0.47	2.26	1.22	1.79	30.34	0.36	6.21	158.86	0.00	26.60	228.10
9.	Water bodies	0.28	0.00	0.08	0.14	0.21	0.01	0.20	0.12	0.49	1.39	2.92
10.	Dry water bodies	3.54	1.66	2.94	0.75	11.06	0.52	5.37	10.97	0.10	27.76	64.68
Total Area 2011		8.83	19.88	19.24	11.09	228.59	5.91	54.57	207.34	0.98	127.41	683.84

Table 8. Change detection matrix from 2001 to 2011 in sq.KM

class No.	class Name	Limestone Mines	Mine waste	Town/Village/Roads/Rails	Industrial area	Fallow land	Crop land	Natural vegetation	Barren land/Hill shade	Water bodies	Dry water bodies	Total Area 2011
1.	Limestone Mines	1.58	0.70	0.33	0.21	1.48	0.08	0.18	0.77	0.16	3.51	9.00
2.	Mine waste	1.16	5.69	2.38	1.05	5.54	0.05	0.31	1.91	0.06	1.74	19.90
3.	Town/Village/Roads/Rails	0.77	0.36	3.31	1.04	5.66	0.88	1.64	2.92	0.08	2.58	19.25
4.	Industrial area	0.17	0.40	0.29	3.00	2.01	0.03	0.08	4.23	0.05	0.82	11.09
5.	Fallow land	0.88	4.57	2.20	1.01	190.66	1.90	2.39	11.45	0.47	13.10	228.61
6.	Crop land	0.01	0.02	0.11	0.10	1.39	2.25	1.16	0.48	0.06	0.34	5.91
7.	Natural vegetation	0.20	0.35	2.87	1.37	18.21	5.40	9.91	9.40	0.63	6.23	54.57
8.	Barren land/Hill shade	0.54	1.99	1.76	0.94	24.26	1.20	4.30	160.46	0.15	12.32	207.92
9.	Water bodies	0.09	0.00	0.00	0.04	0.00	0.07	0.01	0.06	0.57	0.14	0.98
10.	Dry water bodies	0.88	2.60	4.68	1.45	63.45	2.04	5.26	18.93	0.71	27.43	127.41
Total area 2001		6.28	16.67	17.92	10.21	312.65	13.91	25.25	210.61	2.94	68.20	684.64

Table 9. Change detection matrix from 1991 to 2001 in sq.KM

class No.	class Name	Limestone Mines	Mine waste	Town/Village/Roads/Rails	Industrial area	Fallow land	Crop land	Natural vegetation	Barren land/Hill shade	Water bodies	Dry water bodies	Total Area 2001
1.	Limestone Mines	0.91	1.27	0.29	0.15	1.48	0.31	0.08	0.61	0.04	1.15	6.28
2.	Mine waste	0.10	2.59	0.43	0.12	8.33	1.51	0.12	1.05	0.07	2.37	16.67
3.	Town/Village/Roads/Rails	0.18	1.01	3.77	0.21	5.47	0.80	0.80	2.43	0.23	3.03	17.92
4.	Industrial area	0.21	0.69	0.51	1.75	1.84	0.48	0.11	3.10	0.11	1.41	10.21
5.	Fallow land	0.36	2.82	7.36	1.14	200.60	32.93	7.48	23.62	2.43	33.92	312.65
6.	Crop land	0.04	0.10	0.46	0.04	1.92	3.45	3.48	1.96	0.96	1.50	13.91
7.	Natural vegetation	0.06	0.20	2.74	0.06	4.74	2.05	5.47	5.91	0.78	3.23	25.25
8.	Barren land/Hill shade	0.29	1.00	2.47	0.69	14.41	3.22	4.15	174.62	0.50	9.26	210.61
9.	Water bodies	0.05	0.05	0.16	0.08	0.33	0.14	0.31	0.21	1.39	0.23	2.94
10.	Dry water bodies	0.19	0.78	3.26	1.49	21.94	1.77	1.77	13.30	1.09	22.63	68.20
Total area 1991		2.39	10.5	21.45	5.73	261.06	46.64	23.76	226.79	7.60	78.73	684.64

5. Conclusions

The Hybrid classification Technique has merged features of unsupervised and supervised classification, with this classification we are achieved 92% overall *lulc* classification accuracy for the years 1991, 2001, 2011 and 2019, with 0.91 Overall Kappa index. Classified images are dominated by follow lands and Barren lands because of the major cultivation is seasonal rail fall dependent and in the months of April and May scant rainfall record. The results indicate change of *lulc* over the period of 30 years. Limestone mining area increases from 0.35 % (2.39 km²) to 1.64% (11.18km²), Limestone mining waste area increases from 1.53 % (10.50km²) to 3.74% (25.56km²), Industrial area increases from 0.84 % (5.73 km²) to 1.80% (12.31km²). Follow Land decreases from 38.17% (261.07 km²) to 33.28% (227.62km²) and crop land decreases from 6.82 % (46.64 km²) to 4.26% (29.12km²). In this paper Indices are computed to extract training samples and to measure *Land Surface Emissivity (LSE)* and *Land Surface Temperature (LST)* for the three decades of the study area in future work and need to compare classified data with real time data.

Acknowledgements

The author is thankful to the Limestone Mine and Cement industries management for providing permission to carry out fieldwork in the study area. Also, he is grateful to the colleagues for their part in the execution of this work.

Data availability statement

Landsat data (<https://earthexplorer.usgs.gov/>) is obtained from USGS earth explorer website and processed in a ERDAS IMAGINE and ArcGIS in institutional licensed platform.

Conflicts of Interest

Authors would like to make it clear that this publication has no conflicts of interest, and that there has been no financial funding for it that may have affected its outcome.

References

- [1] Haoteng Zhao, Yong Ma, Fu Chen, Jianbo Liu, Liyuan Jiang, Wutao Yao, Jin Yang, "Monitoring Quarry Area with Landsat Long Time-Series for Socioeconomic Study," *Remote Sensing* 10, 517, 2018.
- [2] Imane Bachri, Mustapha Hakdaoui, Mohammed Raji, Ana Cláudia Teodoro, Abdelmajid, Benbouziane. "Machine Learning Algorithms for Automatic Lithological Mapping Using Remote Sensing Data: A Case Study from Souk Arbaa Sahel, Sidi Ifni Inlier, Western Anti-Atlas, Morocco," *ISPRS Int. J. Geo-Inf.*, 8, 248, 2019.
- [3] SA. Raval, "Investigation of mine environmental monitoring with satellite based sensors," Ph.D Thesis., School of Mining Engineering, The University of New South Wales Sydney, Australia, 2011.
- [4] Merugu Suresh, Dr. Kamal Jain, "Change Detection and Estimation of Illegal Mining using Satellite Images." *Proceedings of 2nd International Conference on Innovations in Electronics and Communication Engineering (ICIECE-2013)*, p.246-250, 2013.
- [5] Department of Mines and Geology (Andhra Pradesh), "District Survey Report YSR Kadapa District," Andhra Pradesh Space applications Centre (APSAC) ITE&C Department, Govt. of Andhra Pradesh, 139p, 2018. Available from: <https://www.mines.ap.gov.in/miningportal/downloads/applications/kadapa.pdf>
- [6] A. Chandra Mouli, R.C.Hanumanthu, R.Jagadiswara Rao, "Conflicting Land-Use Practices in the Narji Limestone Belt in YSR District, Andhra Pradesh, India." *Open Access e-Journal Earth Science India- Popular Issue*, V (III), p.1-9. 2012.
- [7] John R Jensen, "Introductory Digital Image Processing- A Remote Sensing Perspective". Pearson series in Geographic information science, 2015. ISBN: 978-0-13-405816-0
- [8] Perpetual Pehrah, "Assessing Land Cover Change Resulting from Surface Mining Development (A Case Study of Prestea and Its Environs in the Western Region of Ghana)," Master of Science Thesis. Kwame Nkrumah University of Science and Technology College of Engineering. 2015.
- [9] C. Kamusoko, M. Aniya, "Hybrid classification of Landsat data and GIS for land use/ cover change analysis of the Bindura district, Zimbabwe," *International Journal of Remote Sensing*, Taylor & Francis, Vol. 30, No. 1, p. 97-115, 2009.
- [10] Lillesand Thomas, W. Kiefer. Ralph, Chipman Jonathan, "Remote

sensing and image interpretation”, John Wiley & Sons. 2015.

- [11] Nur Hidayati Iswari, R.Suharyadi, Projo Danoedoro, “Developing an Extraction Method of Urban Built-Up Area Based on Remote Sensing Imagery Transformation Index.” *Forum Geografi (Indonesian journal of spatial and regional Analysis)*, vol 32(1), p. 96-108, 2018.
- [12] Bona Daniel Sande, Arymurthy Aniasi Mumi, Mursanto Petrus, “Classification of Limestone Mining Site using MultiSensor Remote Sensing Data and OBIA Approach A case study: Biak Island, Papua.” *International Conference on Advanced Computer Science and Information Systems (ICACSIS 2018-IEEE)*:417-422, 2018.
- [13] C.Venkata Sudhakar, G.Umamaheesrara Reddy, “Land use/Land Cover Change Assessment of YSR Kadapa District, Andhra Pradesh, India using IRS Resourcesat-1/2 Liss III Multi-Temporal Open Source Data,” *International Journal of Recent Technology and Engineering (IJRTE)*, Volume-8 Issue-3, September 2019,
- [14] Musa Dalil, Amodu Isaiiah Omeiza, Yahaya Abdullahi Abbas Abdul Husaini, “Effect of cement factory on land use- land cover in Obajana Lokoja Local Government Area, Kogi State, Nigeria.” *African Journal of Environmental Science and Technology*, Vol.11(7),p.384-392,2017 doi: 10.5897/ AJEST2017.2327.
- [15] S.L. Borana, S.K.Yadav, S.K.Parihar, V.S. Palria, “Impact Analysis of Sandstone Mines on Environment and LU/LC Features Using Remote Sensing and GIS Technique: A Case Study of the Jodhpur City, Rajasthan, India,” *Journal of Environmental Research and Development*, Vol. 8 No. 3A, P: 796-804, 2014.
- [16] J.S. Rawat, B.Vivekananda, K.Manish, “Changes in land use/cover using geospatial techniques: A case study of Ramnagar town area,district Nainital, Uttarakhand, India.” *The Egyptian Journal of Remote Sensing and Space Science*, Volume 16, Issue1:111-117, 2013.
- [17] Ujoh Fanan, Alhassan Muhammad Mamman, Ujoh Frederick Terkuma, “Multi-temporal change detection at a limestone mining and cement production facility in Central Nigeria,” *American Journal of Environmental protection*, volume 3(3):113-121,2014.
- [18] D. Lu, Q.Weng, “Survey of image classification methods and techniques for improving classification performance,” *International Journal of Remote Sensing*, vol. 28, no.5:823–870, 2007.
- [19] R.E.Lamare, O.P. Singh “limestone mining and its environmental implications in meghalaya, india.” *ENVIS bulletin himalayan ecology*, vol 24:87-100, 2016.
- [20] Ganapathi Harsh, Phukan Mayuri, ‘Environmental Hazards of Limestone Mining and Adaptive Practices for Environment Management Plan,’ *Environmental Processes and Management*, *Water Science and Technology Library* 91:121-134, 2020.
- [21] Niyomthai Saneh, Wattanawan Annuwat, “Sustainable Mining in Thailand: Paradigm Shift in Environmental Management.” *Applied Environmental Research*, 36 (1): 55-63, 2014.
- [22] R. Vimala, A. Marimuthu, S. Venkateswaran and R. Poongodi, “Unsupervised ISODATA algorithm classification used in the landsat image for predicting the expansion of Salem urban, Tamil Nadu,” *Indian Journal of Science and Technology*; 13(16):1619–1629,2020.
- [23] Anju Asokan, J Anitha, Ciobanu Monica, Andrei Gabor, Antoanela Naaji and D Jude Hemanth, “Image Processing Techniques for Analysis of Satellite Images for Historical Maps Classification—An Overview,” *Applied Science*. 10, 4207,1-21, 2020.